Proceedings of the 11th Brazilian Congress of Thermal Sciences and Engineering -- ENCIT 2006
Braz. Soc. of Mechanical Sciences and Engineering -- ABCM, Curitiba, Brazil,- Dec. 5-8, 2006

Paper CIT06- 0741

SIMULATION OF FLOW PAST AN ABRUPT CONTRACTION WITH A POROUS INSERT USING LINEAR AND NONLINEAR k-ε MODELS

Reinaldo M. Orselli
Cleges Fischer
Marcelo J.S. De-Lemos[1]
Departamento de Energia - IEME
Instituto Tecnológico de Aeronáutica - ITA
12228-900 - São José dos Campos - SP – Brasil
[1] Corresponding author, delemos@ita.br.

Abstract. *This work presents a numerical investigation for the turbulent flow in an abrupt contraction pipe (section area ratio of 0.285) with a porous insert placed past the contraction. The Reynolds number considered is 50,000 based on the pipe inlet diameter. The flow equations are discretized by using the control volume method and the SIMPLE algorithm is applied for the velocity-pressure coupling. Results for the hybrid medium are obtained using linear and nonlinear k-ε macroscopic models. Parameters such as permeability and thickness of the porous insert are varied in order to analyze their effects on the flow pattern. Pressure losses and streamlines results obtained by the two turbulence models are compared for the cases without and with a porous insert. For the cases without porous insert, whereas the minor loss obtained by the linear model over-predicts the experimental data, good agreement was found for the minor loss obtained by the nonlinear model indicating an advantage of the nonlinear closure in predicting more realistic results. For the cases with porous insert, the results show that despite the attenuation or the suppression of the recirculating bubble, the flow losses are always higher in comparison with the cases without porous insert and the losses are significantly more affected by the porous insert permeabity than its thickness.*

Keywords*. Porous Media, Sudden Contraction, Numerical Simulation, Turbulent flow*

1. Introduction

Flow studies in pipes with sudden contraction have been the subject of numerous publications. Streeter (1961) and Rouse (1950) showed experimental values of minor losses as a function of S_{ex}/S_{in}, the ratio between the pipe outlet cross section area (S_{ex}) and its inlet section area (S_{in}), for turbulent flows. Benedict *et al*. (1966) compared experimentally losses considering incompressible and compressible turbulent flows through pipes with abrupt enlargements and contractions, reviewed the basis of the theory concerning the loss coefficients for abrupt enlargements and contractions and discussed some references about the subject. Durst & Loy (1985) investigated laminar flows for S_{ex}/S_{in} = 0.285. In that work, experimental and numerical results for velocity profiles, recirculating bubble dimensions and pressures losses were compared. Ajayi *et al.* (1998) investigated experimentally the effect on the flow losses of a perturbation upstream a pipe sudden contraction (S_{ex}/S_{in} = 0.25) from laminar to moderately high Reynolds numbers. Also, numerical simulations were performed for the cases without upstream perturbation and good agreement between numerical and experimental results was found for the contraction loss coefficient.

Many articles have been recently published in the literature concerning numerical simulations of flows past planar channels with porous insert. In the works of Assato & de Lemos (2002, 2003) and Assato *et. al.* (2005) it was simulated numerically a turbulent flow through a backward-facing step and in Assato & de Lemos (2004a-b) it was simulated the case of a flow past a forward-facing step. In general, these articles showed a comparison of numerical results applying both linear and non-linear turbulence models and in order to analyze the effects of the porous insert on the flow pattern some parameters such as porosity, permeability and thickness were varied. In addition, with regard to this subject, other recent works can be mentioned such as the work of Chan & Lien (2005) where it was examined the influence of permeability, forchheimer's constant and thickness on the flow (turbulent) in a planar channel which suffers a sudden expansion (back-step). And the work of de Lemos & Tofaneli (2003) where it was analyzed the influence of porosity, permeability and Reynolds number on the flow pressure drop in a parallel-plate channel containing porous fins.

Concerning numerical simulations of turbulent flow through an axisymmetric sudden contraction with porous insert, some articles have been recently published such as the works of Orselli & de Lemos (2004, 2005a-c), where, essentially, it was investigated the effect of permeability and thickness on the flow pattern past a sudden contraction pipe with section area ratio of 0.10 and 0.285. And, also, the work of Orselli & de Lemos (2006) where numerical results applying linear and nonlinear turbulence models were shown with a section area ratio of 0.10.

In the present work, numerical results for turbulent flow through a sudden contraction pipe (section area ratio of 0.285) with a porous insert (located past the sudden contraction section) are presented in which both linear and nonlinear eddy viscosity macroscopic models are employed.

Developments of nonlinear eddy viscosity models (NLEVM) have recently been the subject of many publications such as in Speziale (1987), Nisizima & Yoshizawa (1987), Rubinstein & Barton (1990), Shih *et al.* (1993) and Park & Sung (1995). The NLEVM which corresponds to an extension of the linear eddy viscosity models (LEVM) have presented some advantage over the LEVM mainly for flows in which anisotropy of the normal Reynolds stresses is important (Assato & de Lemos, 2000, Wilcox, 1998).

Therefore, in this work, comparisons of results simulated with both linear and nonlinear macroscopic k-ε turbulence models for turbulent flow past a sudden contraction pipe without and with a porous insertion are presented. In addition, parameters such as permeability and thickness of the porous insert are varied in order to analyze particularly its influence on the flow losses and on the damping of the recirculating bubble.

2. Geometry Under Consideration

Figure (1a) shows the geometry under consideration where due to the sudden contraction the flow direction changes abruptly resulting in a recirculating bubble past the contraction section. The recirculating bubble causes a reduction of the effective flow area, phenomenon known as *vena contracta*, whose minimum area is denoted S_c. Figure (1b) presents a sketch of the porous insert in the pipe, the subscripts in and ex represent the pipe inlet and outlet, respectively. In Figs. (1a) and (1b), U_{in} and U_{ex} are the mean velocities at a pipe cross section in the stream-wise direction, l_{in} and l_{ex} are the pipe lengths, d_{in} and d_{ex} or $2\,r_{in}$ and $2\,r_{ex}$ correspond to the diameters and a is the porous insert thickness. In this work, two porous insert thickness are considered which are $a/r_{ex} = 0.083$ and $a/r_{ex} = 0.166$. The adopted section pipe ratio is $S_{ex}/S_{in} = 0.285$ which corresponds to $r_{ex}/r_{in} = 0.534$.

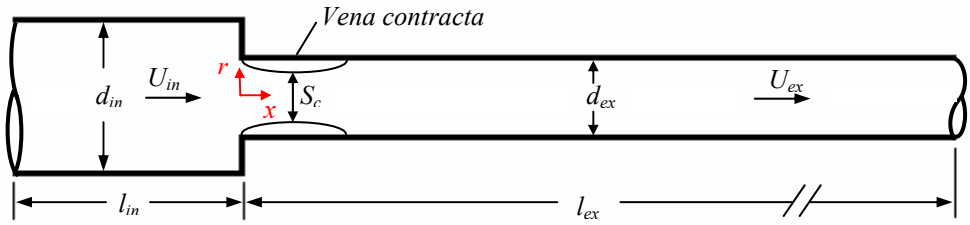

a)

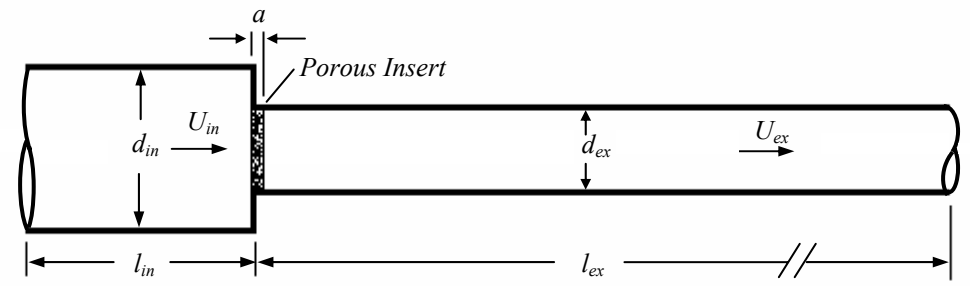

b)

Figure 1. Simple sketch of the pipe geometry: a) *vena contracta*; b) Porous insert.

3. Mathematical Model

The governing equations applied here have already been derived in details, Pedras & de Lemos (2001a-c), and for this reason their derivation need not to be repeated here. Considering the porous medium homogeneous, rigid and saturated in an incompressible single-phase fluid, the macroscopic form of the governing equations is obtained by employing the volumetric average to the time-averaged equations, where this development is based on the concept of double decomposition, de Lemos & Pedras (2001), Pedras & de Lemos (2000).

In the following governing equations, the transient and the gravitational terms are neglected.

The macroscopic continuity equation can be written as,

$$\nabla \cdot \overline{\mathbf{u}}_D = 0 \tag{1}$$

where $\overline{\mathbf{u}}_D$ is the average surface velocity ("seepage" or Darcy velocity). Equation (1) was found by applying the Dupuit-Forchheimer relationship, $\overline{\mathbf{u}}_D = \phi\langle\overline{\mathbf{u}}\rangle^i$, where ϕ is the porous medium porosity and $\langle\overline{\mathbf{u}}\rangle^i$ is the intrinsic (liquid) average of the local velocity vector $\overline{\mathbf{u}}$ (Gray & Lee, 1977).

The macroscopic momentum equation is given by,

$$\rho\nabla\cdot\left(\frac{\overline{\mathbf{u}}_D\,\overline{\mathbf{u}}_D}{\phi}\right) = -\nabla(\phi\langle\overline{p}\rangle^i) + \mu\nabla^2\overline{\mathbf{u}}_D + \nabla\cdot(-\rho\phi\langle\overline{\mathbf{u}'\mathbf{u}'}\rangle^i) - \left[\frac{\mu\phi}{K}\overline{\mathbf{u}}_D + \frac{c_F\phi\rho|\overline{\mathbf{u}}_D|\,\overline{\mathbf{u}}_D}{\sqrt{K}}\right] \tag{2}$$

where the correlation $-\rho\overline{\mathbf{u}'\mathbf{u}'}$ is obtained by employing the time-average operator to the local instantaneous momentum equation. Then, applying the volume-average procedure to the entire momentum equation (see Pedras & de Lemos, 2001a for details), results in the term $-\rho\phi\langle\overline{\mathbf{u}'\mathbf{u}'}\rangle^i$ of Eq. (2). This term is here recalled the Macroscopic Reynolds Stress Tensor (MRST). Then, making use the relationship $\overline{\mathbf{u}}_D = \phi\langle\overline{\mathbf{u}}\rangle^i$, Eq. (2) is finally obtained. The last two terms in the right hand side of Eq. (2) represent the Darcy-Forchheimer contributions where the constant c_F is the Forchheimer coefficient. In addition, the term $\langle\overline{p}\rangle^i$ is the intrinsic average pressure of the fluid, ρ is the fluid density, μ represents the dynamic fluid viscosity and the symbol K corresponds to the porous medium permeability. Also, the equations given are valid for the clear medium as well, setting $\phi = 1$ ($K \to \infty$) and discarding the last two terms.

As proposed by Pedras & de Lemos (2001a), the term MRST is modeled considering a linear stress-strain relationship in analogy with the Boussinesq concept for clear flow case as,

$$-\rho\phi\langle\overline{\mathbf{u}'\mathbf{u}'}\rangle^i = \mu_{t_\phi}\langle\overline{\mathbf{D}}\rangle^v - \frac{2}{3}\phi\rho\langle k\rangle^i\mathbf{I} \tag{3}$$

where $\langle k\rangle^i$ represents the intrinsic average of the turbulent kinetic energy (k) and the term

$$\langle\overline{\mathbf{D}}\rangle^v = \left[\nabla\overline{\mathbf{u}}_D + [\nabla\overline{\mathbf{u}}_D]^T\right] \tag{4}$$

corresponds to the mean macroscopic deformation tensor and $\mathbf{I}$ is the unity tensor. In Eq. (3), the term μ_{t_ϕ} is the macroscopic eddy viscosity which is modeled similarly to case of clear fluid and a proposal for it was presented in Pedras & de Lemos (2001a) as follows,

$$\mu_{t_\phi} = \rho c_\mu \frac{\langle k\rangle^{i2}}{\langle\varepsilon\rangle^i} \tag{5}$$

where $c_\mu = 0.09$ and $\langle\varepsilon\rangle^i$ is the intrinsic average of the dissipation rate of k.

The macroscopic transport equations for $\langle k\rangle^i = \langle\overline{\mathbf{u}'\mathbf{u}'}\rangle^i/2$ and $\langle\varepsilon\rangle^i = \mu\langle\overline{\nabla\mathbf{u}':\left(\nabla\mathbf{u}'\right)^T}\rangle^i/\rho$ in the k-ε High-Reynolds form were proposed in Pedras & de Lemos (2001a) as,

$$\rho\nabla\cdot(\overline{\mathbf{u}}_D\langle k\rangle^i) = \nabla\cdot\left[(\mu + \frac{\mu_{t_\phi}}{\sigma_k})\nabla(\phi\langle k\rangle^i)\right] - \rho\langle\overline{\mathbf{u}'\mathbf{u}'}\rangle^i:\nabla\overline{\mathbf{u}}_D + c_k\rho\frac{\phi\langle k\rangle^i|\overline{\mathbf{u}}_D|}{\sqrt{K}} - \rho\phi\langle\varepsilon\rangle^i \tag{6}$$

$$\rho\nabla.\left(\overline{\mathbf{u}}_D\langle\varepsilon\rangle^i\right) = \nabla.\left[\left(\mu + \frac{\mu_{t_\phi}}{\sigma_\varepsilon}\right)\nabla\left(\phi\langle\varepsilon\rangle^i\right)\right] + c_1\left(-\rho\left\langle\overline{\mathbf{u}'\mathbf{u}'}\right\rangle^i:\nabla\overline{\mathbf{u}}_D\right)\frac{\langle\varepsilon\rangle^i}{\langle k\rangle^i} + c_2c_\kappa\rho\frac{\phi\langle\varepsilon\rangle^i|\overline{\mathbf{u}}_D|}{\sqrt{K}} - c_2\rho\phi\frac{\langle\varepsilon\rangle^{i2}}{\langle k\rangle^i} \tag{7}$$

where $\sigma_k = 1.0$, $\sigma_\varepsilon = 1.33$, $c_1 = 1.44$, $c_2 = 1.92$ are non-dimensional empirical constants and, specially for the porous medium, c_k was found to be equal to 0.28 through numerical calculations by Pedras & de Lemos (2001a-c, 2003).

In this work, numerical results involving nonlinear eddy viscosity models (NLEVMs) are analyzed. Differently from the linear stress-strain rate relationship, Eq. (3), a more general nonlinear constitutive equation is employed. The NLEVMs here adopted is based on the developments of Speziale (1987), Nisizima & Yoshizawa (1987), Rubinstein & Barton (1990), Shih *et al.* (1993) among others. In these works, quadratic products were introduced involving the strain rate and vorticity tensors with different derivations and calibrations for each model. These nonlinear constitutive

relations offer some advantages over the Boussinesq approximation, most notably for flows in which anisotropy of the normal Reynolds stresses plays an important role, for example, in capturing secondary motion in noncircular ducts or in predicting reattachment length for the back-facing step (Wilcox, 1998, Assato & de Lemos, 2000).

The nonlinear macroscopic k-ε turbulence model here analyzed is composed of the same system of equations (1)-(7). The sole difference between both macroscopic models (linear and nonlinear) lies on the macroscopic Reynolds stress expression, brought to the second order. The macroscopic nonlinear stress-strain expression, in the indexed form, is given as follows:

$$
\begin{aligned}
-\rho\phi\langle\overline{u_j' u_j'}\rangle^i = \left(\mu_{t_\phi}\langle\overline{D}_{ij}\rangle^v\right)^L &- \left(c_{1NL}\mu_{t_\phi}\frac{\langle k\rangle^i}{\langle\varepsilon\rangle^i}\left[\langle\overline{D}_{ik}\rangle^v\langle\overline{D}_{kj}\rangle^v - \frac{1}{3}\langle\overline{D}_{kl}\rangle^v\langle\overline{D}_{kl}\rangle^v\delta_{ij}\right]\right)^{NL1} \\
&- \left(c_{2NL}\mu_{t_\phi}\frac{\langle k\rangle^i}{\langle\varepsilon\rangle^i}\left[\langle\overline{\Omega}_{ik}\rangle^v\langle\overline{D}_{kj}\rangle^v + \langle\overline{\Omega}_{jk}\rangle^v\langle\overline{D}_{ki}\rangle^v\right]\right)^{NL2} \\
&- \left(c_{3NL}\mu_{t_\phi}\frac{\langle k\rangle^i}{\langle\varepsilon\rangle^i}\left[\langle\overline{\Omega}_{ik}\rangle^v\langle\overline{\Omega}_{jk}\rangle^v - \frac{1}{3}\langle\overline{\Omega}_{lk}\rangle^v\langle\overline{\Omega}_{lk}\rangle^v\delta_{ij}\right]\right)^{NL1} - \left(\frac{2}{3}\phi\delta_{ij}\rho\langle k\rangle^i\right)^L
\end{aligned}
\tag{8}
$$

where δ_{ij} is Kronecker delta; the superscripts L and NL indicate, respectively, the liner and nonlinear contributions, $\langle\overline{D}_{ij}\rangle^v$ and $\langle\overline{\Omega}_{ik}\rangle^v$ are, respectively, the macroscopic deformation and vorticity tensors which can be written in the indexed form as:

$$
D_{ij} = \left(\frac{\partial u_i}{\partial x_j} + \frac{\partial u_j}{\partial x_i}\right),\ \Omega_{ij} = \left(\frac{\partial u_i}{\partial x_j} - \frac{\partial u_j}{\partial x_i}\right) \tag{9}
$$

The nonlinear model proposed by Shih *et al.* (1993) is here adopted whose non-dimensional constants are given by:

$$
c_\mu = \frac{2/3}{1{,}25 + s + 0{,}9\Omega},\ c_{1NL} = \frac{0{,}75}{c_\mu(1000 + s^3)},\ c_{2NL} = \frac{3{,}8}{c_\mu(1000 + s^3)},\ c_{2NL} = \frac{4{,}8}{c_\mu(1000 + s^3)} \tag{10}
$$

where $s = \langle k\rangle^i/\langle\varepsilon\rangle^i\sqrt{0.5\ \langle\overline{D}_{ij}\rangle^v\langle\overline{D}_{ij}\rangle^v}$ and $\Omega = \langle k\rangle^i/\langle\varepsilon\rangle^i\sqrt{0.5\ \langle\overline{\Omega}_{ij}\rangle^v\langle\overline{\Omega}_{ij}\rangle^v}$.

4. Boundary Conditions and Numerical Details

A developed profile of velocity, k and ε (obtained numerically) was imposed at the pipe inlet cross section, and, at its outlet, it was applied a zero diffusion flux condition. In addition, the classical logarithmic wall function was employed for describing the flow near the wall.

In order to solve numerically the flow equations, it was employed the finite volume method applied to a boundary-fitted coordinate system. Equations were discretized in a bi-dimensional axisymmetric domain involving both the clear and the porous medium. Moreover, the SIMPLE algorithm was used for handling the velocity-pressure coupling, (Patankar, 1980) and residues for all transport equations were brought down to 10^{-6}. For more details about the numerical method implemented, see Pedras & de Lemos (2001b).

In order to verify grid independence on the numerical results, besides the axisymmetric mesh of size 202 x 82 (upstream the pipe contraction) and 924 x 46 (downstream the pipe contraction), two additional grids were generated: a coarser mesh with size of 135 x 52 and 616 x 28 and a refined mesh with size of 267 x 115 and 1233 x 64. The differences between the results given by the two more refined meshes were less than 1% for the contraction minor loss coefficient, k_c, whose definition is presented in the following section. Therefore, the grid of size 202 x 82 and 924 x 46 was considered to be sufficiently refined and Fig. (2) presents a partial view of the grid points distribution at the contraction region where it can be observed a concentration of grid points towards the wall and the contraction corner.

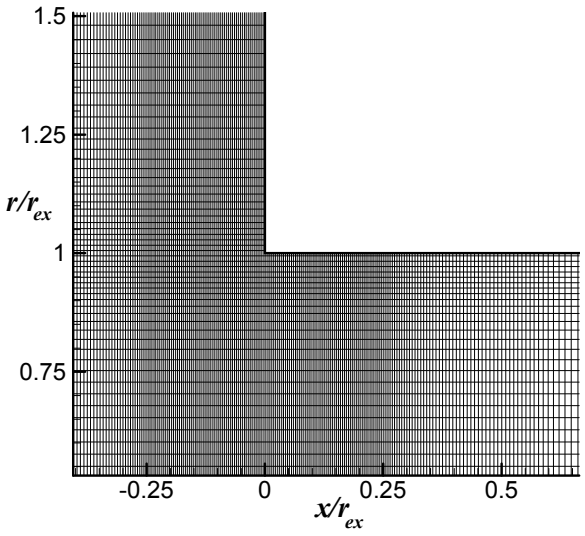

Figure 2. Partial view of the axysimmetric grid at the contraction region: grid size of 202 x 82 (upstream the contraction) and 924 x 46 (downstream the contraction).

5. Results and Discussion

5.1. Clear flow

As presented in Fig. (1), the geometry considered is of a pipe which suffers a sudden contraction whose section area ratio (S_{ex}/S_{in}) is 0.285. In order to have a negligible influence of the inlet and outlet pipe sections on the results, the inlet and outlet pipe length were found to be, respectively, l_{in}/r_{in} = 2.965 and l_{ex}/r_{ex} = 80. Moreover, it was verified that the outlet pipe length was long enough to assume the flow fully developed in its outlet cross section, condition necessary to use Eq. (14) (shown below) and to assure the validity of a zero diffusion flux as a boundary condition at the pipe outlet.

In all results presented in this work, it was adopted an inlet Reynolds number (Re_{in}) of 50,000 based on the pipe inlet diameter (d_{in}) which corresponds to an outlet Reynolds number (Re_{ex}) of 93,627 based on the pipe outlet diameter (d_{ex}). The inlet and the outlet Reynolds number are, respectively, defined as,

$$Re_{in} = \frac{U_{in} d_{in}}{\nu} \tag{11}$$

$$Re_{ex} = \frac{U_{ex} d_{ex}}{\nu} \tag{12}$$

where U_{in} and U_{ex} are the stream-wise bulk velocities, respectively, upstream and downstream the pipe contraction and ν is the kinematic viscosity.

According to the definition given in Fox & McDonald (1998), the minor loss due to the contraction (h_c) can be written as,

$$h_c = k_c \frac{U_{ex}^2}{2} \tag{13}$$

where k_c is the contraction minor loss coefficient which is a non-dimensional parameter. In Streeter (1961) and Rouse (1950), experimental values of k_c without porous insert are presented for several geometries for turbulent flows. It was observed that the experimental values of Streeter (1961) and Rouse (1950) are presented independently of the Reynolds number which indicates that the k_c values are not significantly affected by the Reynolds number for fully turbulent flows. Thus, according to Streeter (1961) and Rouse (1950), the k_c value was found to be, respectively, 0.367 and 0.408 for S_{ex}/S_{in} = 0.285.

According to Fox & McDonald (1998), considering the energy conservation between two cross sections of steady incompressible flow, under the assumption of no external work and uniform pressure and internal energy across the two sections results,

$$h_T = \left(\frac{p_{in}}{\rho} + \alpha_{in} \frac{U_{in}^2}{2} + g z_{in} \right) - \left(\frac{p_{ex}}{\rho} + \alpha_{ex} \frac{U_{ex}^2}{2} + g z_{ex} \right) \tag{14}$$

where h_T is the total head loss between the two sections, p is the pressure in each section, g is the acceleration of gravity, α is the kinetic energy coefficient and z is the coordinate which corresponds to the height level of the pipe section. Subscriptions in and ex represent the inlet and outlet cross section area, respectively. The kinetic energy coefficient, α , is defined as,

$$\alpha = \frac{\frac{1}{S}\int_S \rho \bar{u}^3 dS}{\rho U^3} \tag{15}$$

where $\bar{u}$ is the time average of the local instantaneous velocity in the axial direction.

The major losses, h_l , can be written as a function of the friction factor, f ,

$$h_l = f \frac{l}{d} \frac{U^2}{2} \tag{16}$$

The total head loss is the sum of all major and minor losses and considering the case of a pipe with a sudden contraction, h_T is given by,

$$h_T = h_l + h_c = f_{in} \frac{l_{in}}{d_{in}} \frac{U_{in}^2}{2} + f_{ex} \frac{l_{ex}}{d_{ex}} \frac{U_{ex}^2}{2} + k_c \frac{U_{ex}^2}{2} \tag{17}$$

where, respectively, f_{in} and f_{ex} are the friction factor due to the major losses upstream and downstream the pipe contraction.

We can define the pressure coefficient, Cp , as,

$$Cp = \frac{p - p_{ref}}{\rho U_{ex}^2 / 2} \tag{18}$$

where, p_{ref} is a reference pressure which is, here, assumed to be null, and, p is a local pressure.

Substituting Eq. (17), (18) in Eq. (14), considering fully developed flow at the inlet and outlet pipe cross section and assuming the pipe sections at same height level, the minor loss coefficient can be obtained as,

$$k_c = (Cp_{in} - Cp_{ex}) + \left[\alpha_{in} \left(\frac{U_{in}}{U_{ex}} \right)^2 - \frac{f_{in}}{2} \frac{l_{in}}{r_{in}} \left(\frac{U_{in}}{U_{ex}} \right)^2 - \frac{f_{ex}}{2} \frac{l_{ex}}{r_{ex}} - \alpha_{ex} \right] \tag{19}$$

where the last four terms (between square brackets) depend only on the pipe geometry, the Reynolds number and the friction factor of the corresponding developed flow. Therefore, they do not vary in the cases, here, analyzed. Thus, the k_c value depends only on the pressure coefficient difference ($Cp_{in} - Cp_{ex}$) between the pipe inlet and outlet cross sections.

In Eq. (19), the values of α_{in} and f_{in} were obtained through a numerical simulation, for Re = 50,000, in a pipe with only the pipe inlet diameter (d_{in}), where a periodic condition between its inlet and outlet was employed. The values of f_{ex} were obtained applying the same periodic conditions but with the outlet pipe diameter (d_{ex}) and Re = 93,627. In addition, the values of α_{ex} were calculated by employing its definition given by Eq. (15) at the pipe outlet section. Table (1) presents the values of $Cp_{in} - Cp_{ex}$, α_{in} , α_{ex} , f_{in} and f_{ex} which were obtained through the

numerical simulations using both the linear and nonlinear macroscopic k - ε turbulence models. Then, making use of Eq. (19), the k_c values can be calculated which are presented in Table (2).

Table 1 - Values of Eq. (19) obtained from the numerical simulations.

Macroscopic k - ε turbulence model	$Cp_{in} - Cp_{ex}$	α_{in}	α_{ex}	f_{in}	f_{ex}
Linear	2.180	1.062	1.057	0.02097	0.01836
Nonlinear	2.063	1.063	1.056	0.02054	0.01796

Table 2 - Values of k_c obtained from the numerical calculations for the case without porous insert.

Macroscopic k - ε turbulence model	k_c	Deviation from experimental value of k_c = 0.367 (Streeter, 1961)	Deviation from experimental value of k_c = 0.408 (Rouse, 1950)
Linear	0.473	28.8 %	15.8 %
Nonlinear	0.373	1.5 %	-8.7 %

According to the results presented in Table (2), it is noted that the nonlinear macroscopic k - ε turbulence model predicts well the experimental values of k_c while the linear one over-predicts their values. These results confirm (as demonstrated in the literature – Wilcox, 1998 and Assato & de Lemos, 2000) the better performance of the nonlinear eddy viscosity model (NLEVM) over the linear one for flows characterized by high streamlines curvatures and separation which is the case here analyzed.

In Fig. (3), it is shown the streamlines numerical results of the flow in the pipe for the case without porous insert which were obtained by applying both the linear (Fig. 3a) and nonlinear (Fig. 3b) k - ε turbulence models. Comparing the streamlines results given by the two turbulence models, it is clearly observed that the recirculating bubble size of the nonlinear model is considerably greater than the one obtained by the linear model indicating that, in this case, the anisotropy of the normal Reynolds stresses (predicted by the nonlinear model) affects significantly the streamlines results. In Figs. (3a) and (3b), it is observed an area surrounded by dashed lines which corresponds to the region used to present the streamlines results of Figs. (4) and (5) in the following subsection.

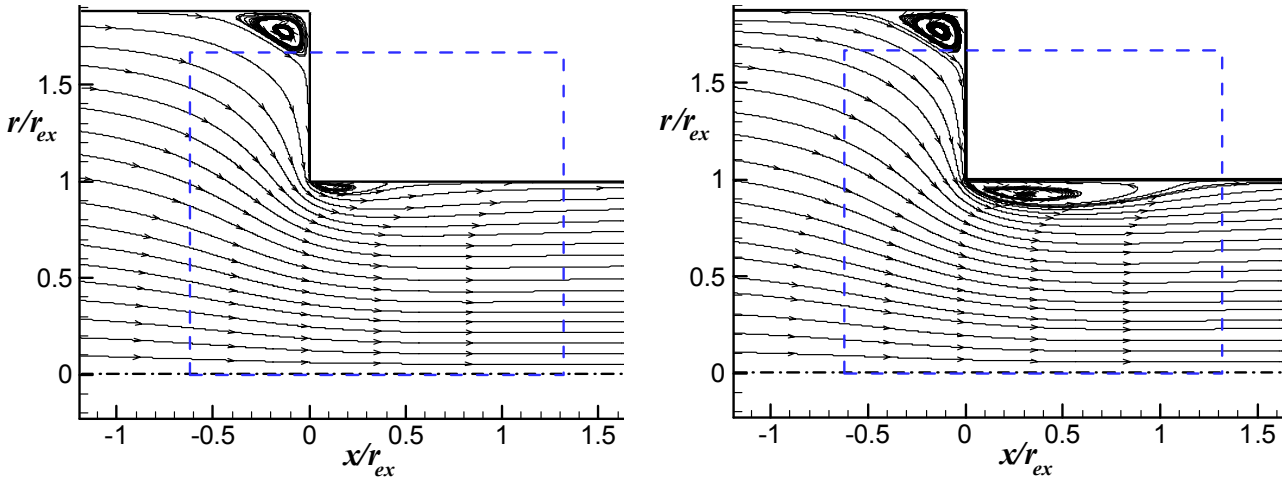

(a) (b)

Figure 3. Streamlines numerical results of the flow in the pipe without porous insert showing an area surrounded by dashed lines to be used in the results of Figs. (4) and (5): a) linear k - ε turbulence model; b) nonlinear k - ε turbulence model.

5.2. Porous insert

Concerning the flow in a pipe with a sudden contraction for the case without porous insert, the recirculating bubble which reduces the effective flow area (*vena contracta*) is the main cause of the minor loss due to the contraction. Therefore, one of the objectives of the porous insert is to suppress or reduce the recirculating bubble, although the porous insert itself increases the losses. This way, there is a compromise between the losses caused by the porous insert and the gain in eliminating or damping the recirculating bubble. Moreover, the numerical results given by both

nonlinear and linear macroscopic eddy viscosity models are compared in order to asses their influence on the flow behavior.

In this subsection, it is presented the numerical results of the flow past a sudden contraction pipe with a porous insert. Concerning the porous insert properties, it was considered two different thicknesses ($a/r_{ex}=0.083$ and $a/r_{ex}=0.166$), a porosity of $\phi=0.85$ and three values of permeability represented by the Darcy Number ($Da=8.56x10^{-3}$, $Da=8.56x10^{-5}$, $Da=8.56x10^{-7}$) which makes 6 different porous insertions. The Darcy number is a non-dimensional parameter related to the permeability (K) whose definition is given by,

$$Da=\frac{K}{(d_{ex})^2} \tag{20}$$

From the numerical simulations, the values of k_c were calculated for each porous insert considered, using both linear and nonlinear macroscopic turbulence models, whose results are presented in Tab. (3).

Table 3 - k_c numerical values for each porous insert, $\phi=0.85$

Macroscopic k - ε turbulence model	a/r_{ex}	Da	k_c
Linear	0	-	0.473
	0.083	8.56×10^{-3}	1.05
		8.56×10^{-5}	5.46
		8.56×10^{-7}	50.07
	0.166	8.56×10^{-3}	1.54
		8.56×10^{-5}	10.41
		8.56×10^{-7}	100.45
Nonlinear	0	-	0.373
	0.083	8.56×10^{-3}	1.02
		8.56×10^{-5}	5.39
		8.56×10^{-7}	50.02
	0.166	8.56×10^{-3}	1.53
		8.56×10^{-5}	10.34
		8.56×10^{-7}	100.41

According to the results of k_c presented in Table (3), it is noted an increase of the minor flow losses in the pipe for lower Darcy values and, also, for higher porous insert thicknesses, being the losses significantly more affected by the Darcy number than the porous insert thickness. Moreover, as the minor losses increase, the differences between the k_c values obtained by the linear and the nonlinear turbulence models become less pronounced. Therefore, the addition of nonlinear terms on the stress-strain expression (resulting in more computing cost) makes little difference on the minor losses results for the cases where the porous insert effect on the flow is more significant (cases with lower Darcy values and higher porous insert thicknesses).

Figures (4) and (5) presents the streamlines numerical results obtained through the linear and the nonlinear k - ε macroscopic turbulence models for the cases without porous insert and with each of the 6 porous inserts considered. In addition, the two vertical lines observed in Figs. (4) and (5) correspond to the upstream and downstream porous insert interfaces. According to the streamlines results of Figs. (4) and (5), it is noticed that the recirculating bubble is significantly damped for $Da=8.56x10^{-3}$ and it is completely suppressed for $Da=8.56x10^{-5}$ and $Da=8.56x10^{-7}$. Moreover, for the cases with $Da=8.56x10^{-5}$ and $Da=8.56x10^{-7}$, it is observed nearly no difference on the streamlines results given by the linear and the nonlinear turbulence models. A possible explanation for this behavior is that the porous insert effect on the flow, which tends to flatten the Darcy velocities profiles, is more dominant than the influence of both the linear and nonlinear approaches given to the macroscopic Reynolds stress tensor. Nevertheless, when $Da=8.56x10^{-3}$, it can be observed that the recirculating bubble predicted by the nonlinear turbulence model is significantly greater than the one obtained by the linear turbulence model which indicates, in this case, that the added nonlinear terms of the turbulence model still have a prominent influence, despite the porous insert effects, on the flow behavior.

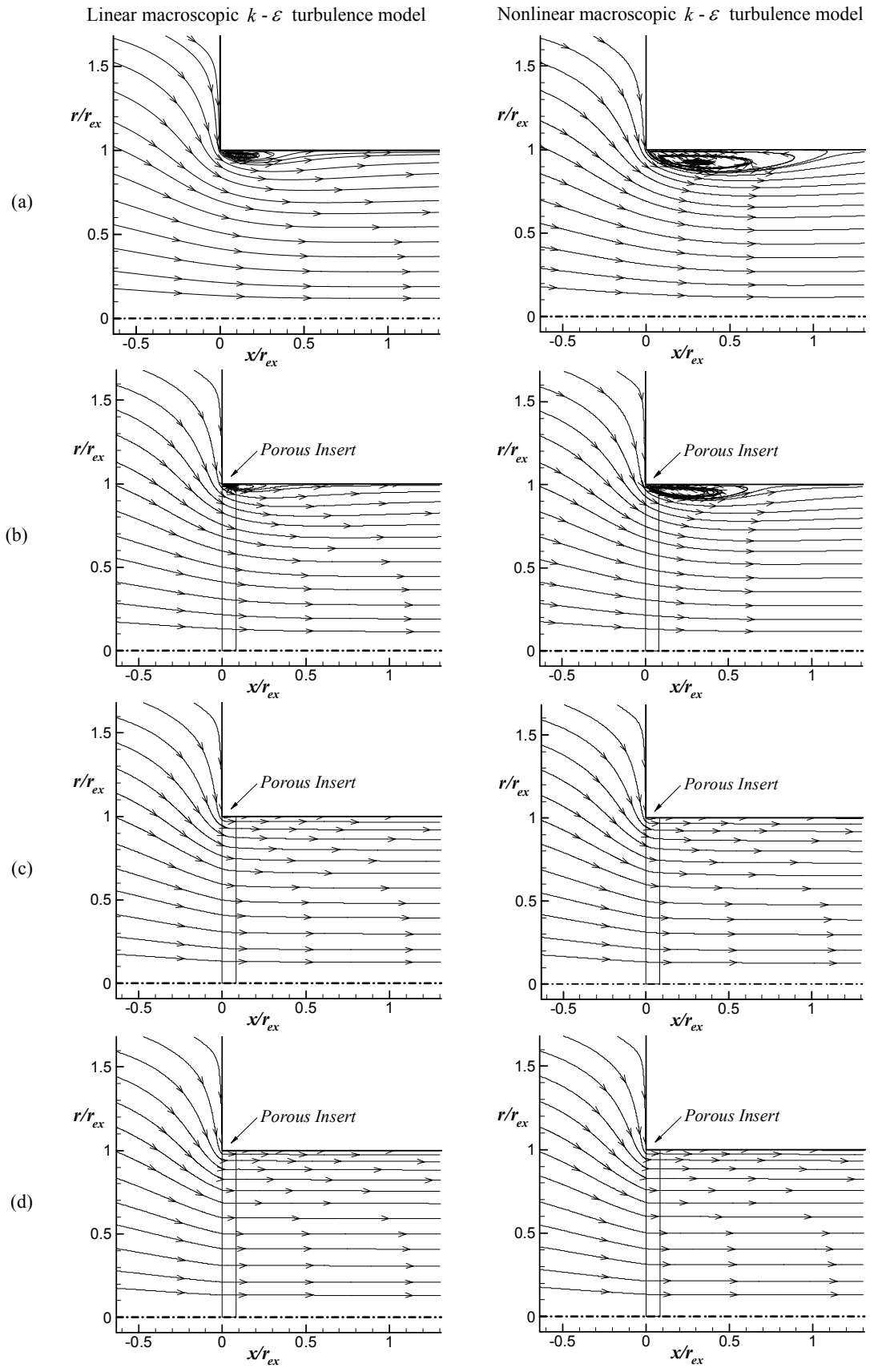

Figure 4. Comparison of streamlines between the linear and nonlinear macroscopic $k-\varepsilon$ turbulence models for $a/r_{ex} = 0.083$ ($\phi = 0.85$): (a) Without porous insert; (b) $Da = 8.56x10^{-3}$; (c) $Da = 8.56x10^{-5}$; (d) $Da = 8.56x10^{-7}$.

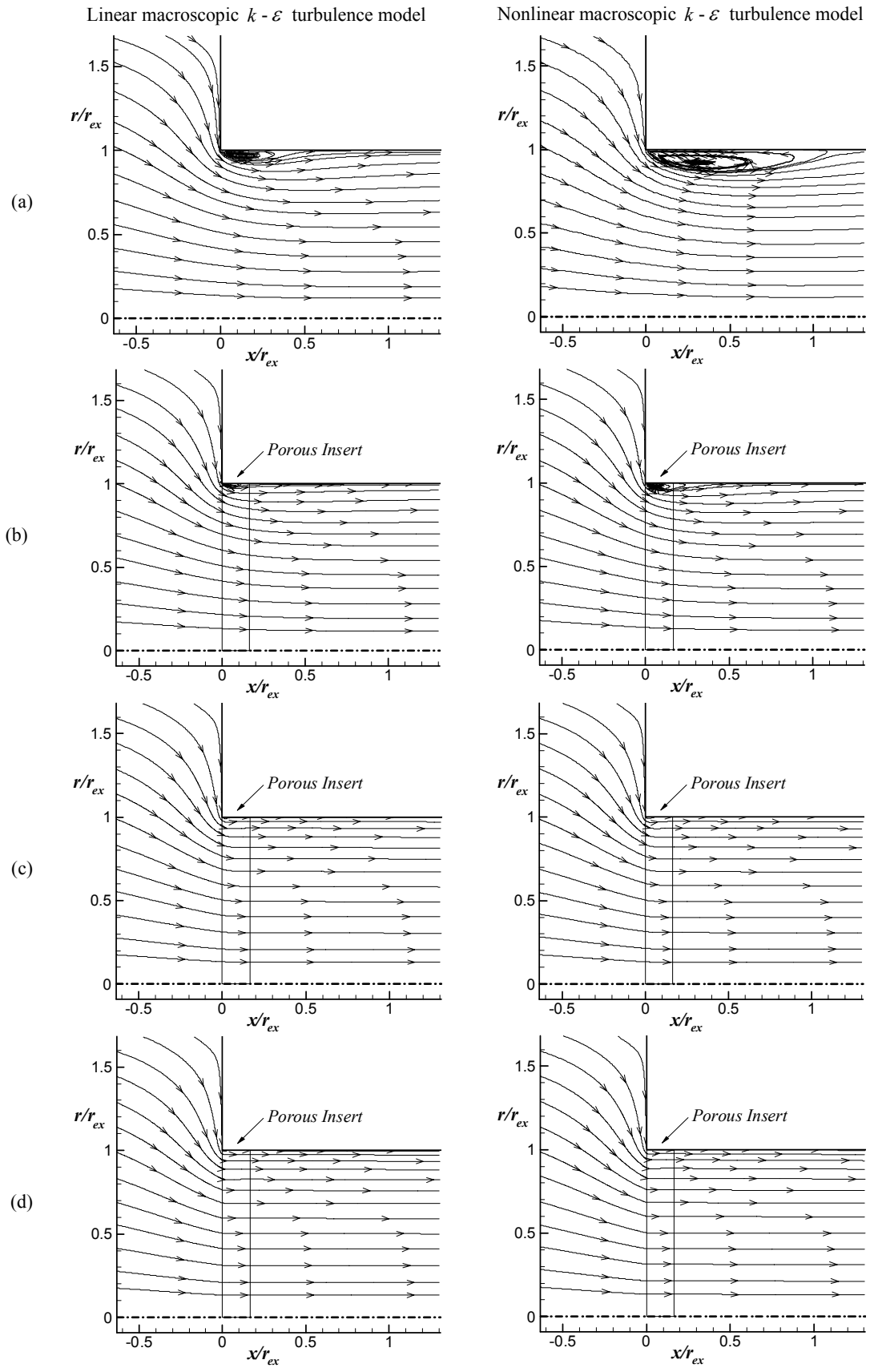

Figure 5. Comparison of streamlines between the linear and nonlinear macroscopic $k-\varepsilon$ turbulence models for $a/r_{ex} = 0.166$ ($\phi = 0.85$): (a) Without porous insert; (b) $Da = 8.56x10^{-3}$; (c) $Da = 8.56x10^{-5}$; (d) $Da = 8.56x10^{-7}$.

6. Conclusion

In this article, both linear and nonlinear turbulence models were applied for simulating the flow past a sudden contraction pipe with a porous insert. In order to asses the effects of the porous insert properties on the flow pattern, parameters such as Darcy number and thickness were varied.

In order to validate the numerical results, the obtained k_c values for the case without porous insert were compared with the experimental ones of Streeter (1961) and Rouse (1950). Whereas the k_c numerical value given by the linear turbulence model over-predicts the experimental data, good agreement was found for the k_c value given by the nonlinear model indicating an advantage of nonlinear closure in predicting more realistic results.

Figures (3)-(5) showed that the recirculating bubble predicted by the linear model was always shorter than the one obtained by the nonlinear model. In addition, it was noted that as the Darcy values decreased and as the porous insert thicknesses increased, the differences between the results obtained by the two turbulence models became less pronounced indicating that the greater the effect of the porous insert on the flow, the lower the influence of the turbulence model on the results.

Moreover, it was observed that the damping of the recirculating bubble and the increase of the flow losses were more affected by the Da values than by the porous insert thicknesses. In addition, no recirculating bubble was observed for $Da = 8.56x10^{-5}$ and $Da = 8.56x10^{-7}$, regardless of the turbulence model used.

Finally, results showed that the minor losses for the cases with porous insert were always higher than the case without porous insert despite the reduction of the recirculating bubble size which indicates that the losses caused by the porous insert itself are more significant than the gain due to the damping of the recirculating bubble. In spite of it, the effect of the permeability and thickness of the porous insert on the flow behavior was analyzed whose findings may be useful in the design of thermo-mechanical equipments, for instance, in the optimization of the heat exchange downstream the pipe contraction section as showed for a forward-facing step geometry in Assato & de Lemos (2004a-b).

7. Acknowledgement

The authors are thankful to CNPq and FAPESP, Brazil, for their financial support during the course of this research.

8. References

Ajayi, K. T., Papadopoulos, G. & Durst, F., 1998, " Influence of upstream development on the losses incurred by flow past an axysymmetric sudden contraction", Proc. 36th Aerospace Sciences Meeting and Exhibit, AIAA-98-0794, Reno, USA.

Assato, M. & de Lemos, M.J.S., 2000, "Tratamento numérico e aplicações de um modelo de viscosidade turbulenta não linear para alto e baixo Reynolds" (in portuguese), Escola Brasileira de Primavera Transição e Turbulência, Uberlândia, Brazil, pp. 459-483.

Assato, A., M. & de Lemos, M.J.S, 2002, "Heat transfer in a suddenly expanded turbulent flow past a porous insert using linear and non-linear eddy-viscosity models", Proc. ASME Int. Mechanical Eng. Congress and Exposition, IMECE2002-39402, New Orleans, USA.

Assato, M. & de Lemos, M.J.S., 2003, "Heat transfer in a back-step flow past a porous insert using a Non-Linear Turbulence model and a Low Reynolds wall treatment", Proc. 3rd Int. Conf. on Computational Heat and Mass Transfer, on CD-ROM, Univ. of Calgary, Banff, Canada.

Assato, M. & de Lemos, M.J.S., 2004a, "Estudo da transferência de calor turbulenta em uma contração abrupta com inserto poroso usando modelos de turbulência linear e não linear" (in Portuguese), Proc. 10th Brazilian Cong. of Thermal Sciences and Engineering, on CD-ROM, Rio de Janeiro, Brazil.

Assato, M. & de Lemos, M.J.S., 2004b, "Flow and heat transfer past a sudden contraction with a porous insert using linear and non-linear turbulence models", Proc. ASME Int. Mechanical Eng. Congress and Exposition, IMECE2004-62407, Anaheim, USA.

Assato, M., Pedras, M.H.J. & de Lemos, M.J.S., 2005, "Numerical solution of turbulent flow past a backward-facing-step with a porous insert using linear and non-linear k-ε models", J.Porous Media, Vol. 8, No.1, pp.13-29.

Benedict R.P., Carlucci, N.A. & Swetz, S.D., 1966, "Flow Losses in abrupt enlargements and contractions", Journal of Engineering for Power, Transactions of ASME, Vol. 88, pp. 73-81.

Chan, C.C. & Lien, F-S, 2005, "Permeability effects of turbulent flow through a porous insert in a backward-facing-step channel, Transport in Porous Media", Vol. 59, No. 1, pp. 47-71.

Durst, F. & Loy, T., 1985, "Investigations of laminar flow in a pipe with sudden contraction of cross section area", Comp. & Fluids, Vol. 13, no. 1, pp. 15-36.

de Lemos, M.J.S. & Pedras, M.H.J., 2001, "Recent mathematical models for turbulent flow in saturated rigid porous media", J. Fluids Eng., Vol. 123, pp. 935-940.

de Lemos, M.J.S & Tofaneli, L.A., 2003, "Pressure drop characteristics of parallel-plate channel flow with porous obstructions at both walls", Proc. ASME Int. Mechanical Eng. Congress and Exposition, IMECE2003-41453, Washington, USA.

Fox, R. W. & McDonald, A. T., 1998, "Introduction to Fluid Mechanics", 5th ed., John Wiley & Sons, New York.

Gray, W.G., Lee, P.C.Y., 1977, "On the theorems for local volume averaging of multiphase system", Int. J. Multiphase Flow, Vol.12, pp.401-410.

Nisizima, S. & Yoshizawa, A., 1987, "Turbulent channel and Couette flows using an anisotropic k - ε model, AIAA J., Vol. 25, No. 3, pp. 414-420.

Orselli, R.M. & de Lemos, M.J.S, 2004, "Escoamento turbulento em contração súbita com inserto poroso" (in portuguese), Proc. 10th Braz. Cong. Thermal Sciences Eng., on CD-ROM, Rio de Janeiro, Brazil.

Orselli, R.M. & de Lemos, M.J.S, 2005a, "Sudden contraction in a turbulent flow with a porous insert, Latin American Journal of Solids and Structures", Vol. 2, No. 3, pp. 269-290.

Orselli, R.M. & de Lemos, M.J.S, 2005b, "Sudden contraction in a turbulent flow with a porous insert using the macroscopic Low Reynolds model", Proc. XXVI Iberian Latin-American Cong. Comp. Meth. Eng., on CD-ROM, Guarapari, Brazil".

Orselli, R.M. & de Lemos, M.J.S., 2005c, "Simulation of turbulent in a sudden contraction with a porous insert", Proc. 18th Int. Cong. Mechanical Engineering, on CD-ROM, Ouro Preto, Brazil.

Orselli, R.M. & de Lemos, M.J.S., 2006, "Simulation of flow past a sudden contraction with a porous insert using linear and nonlinear k - ε models", Proc. XXVII Iberian Latin-American Cong. Comp. Meth. Eng., Belém, Brazil.

Park, T. S. & Sung, H. J., 1995, "A nonlinear low-Reynolds-number k-epsilon model for turbulent separated and reattaching flows", Int. J. Heat and Mass Transfer, Vol. 8, pp. 2657-2666.

Patankar, S.V., 1980, "Numerical heat transfer and fluid flow", Mc-Graw Hill, Hemisphere.

Pedras, M.H.J. & de Lemos, M.J.S., 2000, "On the definition of turbulent kinetic energy for flow in porous media", Int. Commun. Heat and Mass Transfer, Vol. 27, No. 2, pp. 211-220.

Pedras, M.H.J. & de Lemos, M.J.S., 2001a, "Macroscopic turbulence modeling for incompressible flow through undeformable porous media", Int. J. Heat Mass Transfer, Vol. 44, No. 6, pp. 1081-1093.

Pedras, M.H.J. & de Lemos, M.J.S., 2001b, "Simulation of turbulent flow in porous media using a spatially periodic array and a Low Re Two-Equation closure", Numerical Heat Transfer - Part A Appl., Vol. 39, No. 1, pp. 35-59.

Pedras, M.H.J. & de Lemos, M.J.S., 2001c, "On the mathematical description and simulation of turbulent flow in a porous media formed by an array of elleptic rods", J. Fluids Eng., Vol. 123, No.4, pp.941-947.

Pedras, M. H. J. & de Lemos, M.J.S., 2003, "Computational of turbulent flow in porous media using a Low-Reynolds k - ε model and an infinite array of transversally displaced elliptic rods", Numerical Heat Transfer – Part A Appl., Vol. 43, No.1, pp. 585-602.

Rouse, H., 1950, "Enginnering Hydraulics", John Wiley & Sons, New York.

Rubinstein, R. & Barton, J. M., 1990, "Renormalization group analysis of the stress transport equation", Phys. Fluids A, Vol. 2, No. 8, pp. 1472-1476.

Shih, T. H., Zhu, J & Lumley, J. L., 1993, "A Realizable Reynolds Stress Algebraic equation model", NASA TM-105993.

Speziale, C.G., 1987, "On non-linear k - and - models of turbulence", J. Fluid Mech., Vol. 176, pp. 459-475.

Streeter, V.L., 1961, ed., "Handbook of Fluid Dynamics", McGraw-Hill, New York.

Wilcox, D. C., 1998, "Turbulence modeling for CFD", 2nd ed. La Canada: DCW Ind.

9. Copyright Notice